Different subpopulations of kidney interstitial cells produce erythropoietin and factors supporting tissue oxygenation in response to hypoxia in vivo

Broeker, Katharina A E ; Fuchs, Michaela A A ; Schrankl, Julia ; Kurt, Birgül ; Nolan, Karen A ; Wenger, Roland H ; Kramann, Rafael ; Wagner, Charlotte ; Kurtz, Armin

Abstract: Genetic induction of hypoxia signaling by deletion of the von Hippel-Lindau (Vhl) protein in mesenchymal PDGFR- + cells leads to abundant HIF-2 dependent erythropoietin (EPO) expression in the cortex and outer medulla of the kidney. This rather unique feature of kidney PDGFR- + cells promote questions about their special characteristics and general functional response to hypoxia. To address these issues, we characterized kidney PDGFR- + EPO expressing cells based on additional cell markers and their gene expression profile in response to hypoxia signaling induced by targeted deletion of Vhl or exposure to low oxygen and carbon monoxide respectively, and after unilateral ureteral obstruction. CD73+, Gli1+, tenascin C+ and interstitial SMMHC+ cells were identified as zonally distributed subpopulations of PDGFR- + cells. EPO expression could be induced by Vhl deletion in all PDGFR- + subpopulations. Under hypoxemic conditions, recruited EPO+ cells were mostly part of the CD73+ subpopulation. Besides EPO production, expression of adrenomedullin and regulator of G-protein signaling 4 was upregulated in PDGFR- + subpopulations in response to the different hypoxic stimuli. Thus, different kidney interstitial PDGFR- + subpopulations exist, capable of producing EPO in response to different stimuli. Activation of hypoxia signaling in these cells also induces factors likely contributing to improved kidney interstitial tissue oxygenation.

DOI: https://doi.org/10.1016/j.kint.2020.04.040

Different subpopulations of kidney interstitial cells produce erythropoietin and factors supporting tissue oxygenation in response to hypoxia *in vivo*

OPEN

Katharina A.E. Broeker[1], Michaela A.A. Fuchs[1], Julia Schrankl[1], Birgül Kurt[1], Karen A. Nolan[2], Roland H. Wenger[2], Rafael Kramann[3], Charlotte Wagner[1] and Armin Kurtz[1]

[1]*Institute of Physiology, University of Regensburg, Regensburg, Germany;* [2]*Institute of Physiology and National Centre of Competence in Research "Kidney.CH," University of Zürich, Zürich, Switzerland; and* [3]*Department of Nephrology and Clinical Immunology, RWTH Aachen, Aachen, Germany*

Genetic induction of hypoxia signaling by deletion of the von Hippel-Lindau (Vhl) protein in mesenchymal PDGFR-β^+ cells leads to abundant HIF-2 dependent erythropoietin (EPO) expression in the cortex and outer medulla of the kidney. This rather unique feature of kidney PDGFR-β^+ cells promote questions about their special characteristics and general functional response to hypoxia. To address these issues, we characterized kidney PDGFR-β^+ EPO expressing cells based on additional cell markers and their gene expression profile in response to hypoxia signaling induced by targeted deletion of Vhl or exposure to low oxygen and carbon monoxide respectively, and after unilateral ureteral obstruction. CD73$^+$, Gli1$^+$, tenascin C$^+$ and interstitial SMMHC$^+$ cells were identified as zonally distributed subpopulations of PDGFR-β^+ cells. EPO expression could be induced by Vhl deletion in all PDGFR-β^+ subpopulations. Under hypoxemic conditions, recruited EPO$^+$ cells were mostly part of the CD73$^+$ subpopulation. Besides EPO production, expression of adrenomedullin and regulator of G-protein signaling 4 was upregulated in PDGFR-β^+ subpopulations in response to the different hypoxic stimuli. Thus, different kidney interstitial PDGFR-β^+ subpopulations exist, capable of producing EPO in response to different stimuli. Activation of hypoxia signaling in these cells also induces factors likely contributing to improved kidney interstitial tissue oxygenation.

Kidney International (2020) **98,** 918–931; https://doi.org/10.1016/j.kint.2020.04.040

KEYWORDS: erythropoietin; hypoxia; PDGFR-β; renal injury; renal interstitial cells; tissue oxygenation

Correspondence: *Katharina A.E. Broeker, Institute of Physiology, University of Regensburg, Universitätsstraße 31, D-93053 Regensburg, Germany. E-mail: Katharina.Gerl@ur.de*

Received 8 July 2019; revised 30 March 2020; accepted 2 April 2020; published online 23 May 2020

Translational Statement

Tissue oxygenation is dependent on proper erythropoietin (EPO) production and local regulatory factors. We investigated different subpopulations of possible EPO-producing cells in the mouse kidney under hypoxemic stimuli and experimental kidney fibrosis. These cells comprise a heterogeneous group of interstitial cells, which share the expression of PDGFR-β. Induction of hypoxia signaling in these cells induces the expression of factors supporting tissue oxygenation. These data could provide a starting point for closer investigations of the fine regulation of tissue oxygenation. In addition, the here-defined subpopulations of PDGFR-β^+ interstitial cells could present new targets for a pharmacologic approach to treat EPO deficiency.

The kidneys are the main site of oxygen-regulated erythropoietin (EPO) production. Within the kidneys, tubulointerstitial cells produce EPO[1,2] triggered by hypoxia inducible factor 2 (HIF-2).[3] The regulation of renal EPO production occurs mainly by recruitment of EPO-producing cells that express EPO in an on/off fashion.[4] In the normoxic kidney, few EPO-expressing cells are found at the boundary between cortex and outer medulla (OM), whereas under severe hypoxic stress, EPO-expressing cells are recruited in the whole cortex and OM.[5–7] The identity and functional characteristics of those active and potentially EPO-producing cells are less clear. Originally, EPO-producing cells had been identified as interstitial fibroblast-like cells expressing CD73 (ecto-5′-nucleotidase).[1] More recent studies have suggested that in addition to CD73$^+$ cells, also other cell types are able to express EPO.[8] Such a heterogeneity of renal EPO-producing cells has also been suggested by data from mice lacking HIF prolyl-4-hydroxylases in renal stroma cell precursors[9] and has received support by the concept that EPO-producing cells could be telocytes[10] or pericytes.[11] EPO-producing cells have a stellate form with multiple extensions such as pericytes,[10,12,13] and they are located directly adjacent to capillaries.[1,5,12] Moreover, pericytes are key players in renal fibrosis.[11] Potential EPO-producing cells are the precursors

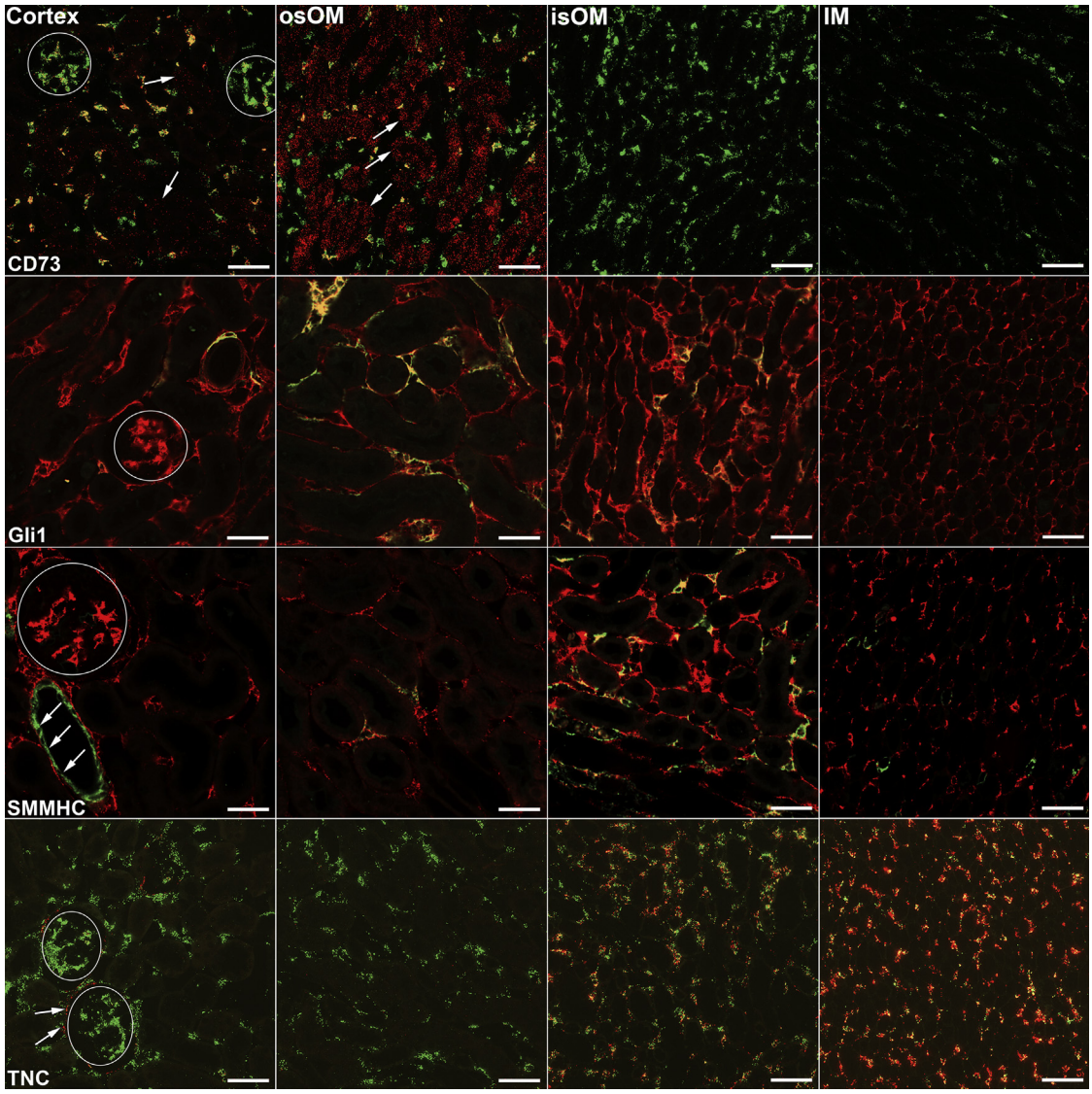

Figure 1 | Localization of PDGFR-β^{+} cells and additional markers on mouse kidney sections in different kidney zones. Interstitial PDGFR-β^{+} cells were distributed over all kidney zones (green in top and bottom row, red in middle rows), with the highest number in the cortex. Intraglomerular mesangial cells were also positive for PDGFR-β. Bars = 50 μm. Top row: a strong colocalization for CD73 (red) and PDGFR-β (green) mRNA could be detected in interstitial cells of the cortex and the outer stripe of the outer medulla (osOM), but not in the inner stripe of the outer medulla (isOM) or inner medulla (IM). CD73 expression was also found in mesangial cells and proximal tubular cells (arrows). Second row: immunohistochemical staining for green fluorescent protein (GFP) (green) and PDGFR-β (red) on a Gli1$^{CreERT2/+}$ mT/mG kidney section. The Gli1-GFP signal was located in cortical and outer medullary interstitial cells and colocalized with PDGFR-β in yellow-appearing cells. Gli1-GFP/PDGFR-β colocalization was almost undetectable in the IM. Third row: immunohistochemical staining for SMMHC-driven GFP (green) on a kidney section of an SMMHC$^{CreERT2/+}$ mT/mG mouse. Colocalization of SMMHC-GFP (green) and PDGFR-β (red) was detectable in approximately 10% of all interstitial PDGFR-β^{+} cells in the OM, especially in the isOM. In the cortex and in the IM, colocalization was very low. Bottom row: *in situ* hybridization for tenascin C (TNC; red) and PDGFR-β (green) mRNA. In the cortex, coexpression in interstitial cells was very low (<5%), but TNC expression could be detected around glomeruli (arrows), presumably in the Bowman's capsules. Colocalization in the osOM was also very low (<5%). In the isOM, colocalization increased to 65% and to 100% in the IM. To optimize viewing of this image, please see the online version of this article at www.kidney-international.org/.

of myofibroblasts in the kidney[14] and the ability of the kidneys to produce EPO ceases with interstitial myofibroblast formation in states of kidney fibrosis.[12,15–17] This concept of EPO-producing cells being pericytes, however, is somewhat contradicted by the fact that classical pericytes are located mainly in the OM and to a lesser extent in the cortex.[18] The pericyte concept is also questioned by the finding that HIF stabilization in cells expressing the fibroblast cell marker PDGFR-β[19] strongly induces EPO expression in the interstitium of the cortex and the OM,[13] whereas HIF stabilization in cells expressing the pericyte marker NG2[19] only negligibly induces EPO expression in the kidney.[20] All renal cells with inducible EPO expression appear to express PDGFR-β, thus defining PDGFR-β as an essential marker of renal EPO-

Table 1 | An overview of the degree of colocalization between PDGFR-β and the respective second markers as well as the colocalization between the additional markers among each other

Cell population	CD73	Gli1	SMMHC	TNC
PDGFR-β	60	15	10	25
CD73	—	15	0	0
Gli1	60	—	5	5
SMMHC	0	8	—	5
TNC	0	3	2	—
EPO in Vhl-KO mice	75	<5	5	10

EPO, erythropoietin; TNC, tenascin C.
All numbers are percentages.
First row: percentage of different subpopulations regarding interstitial PDGFR-β+ cells. Rows 2–5: percentage of colocalization of different subpopulations among each other. To calculate the percentage for the colocalization between different subpopulations, the respective subpopulation named in the left column was set to 100%. For example, 15% of all CD73+/PDGFR-β+ interstitial cells also expressed Gli1, but there was no colocalization between CD73 and SMMHC or TNC, respectively. Last row: percentage of different subpopulations on PDGFR-β+ EPO-producing cells in Vhl-KO mice.

producing cells.[13] PDGFR-β+ cells exist in all organs but physiologically regulated EPO production in these cells appears to be restricted to the kidneys and the brain.[13,20] The restriction of EPO expression to the kidneys is likely not the result of organ-specific differences of oxygen sensing, but is rather due to the selective ability of renal PDGFR-β+ cells to express EPO. This assumption is supported by the finding that cell-type–specific stabilization of HIF-proteins in PDGFR-β+ cells by deletion of the ubiquitin ligase von Hippel-Lindau induces EPO expression substantially only in the kidneys (and to a low degree also in adrenal glands).[13] This organ specificity of EPO expression raised the question about other structural and functional characteristics of renal EPO-producing PDGFR-β+ cells.

So far, different tubulointerstitial cell types have been identified: cells specifically expressing CD73,[1,2] the mesenchymal progenitor cell marker Gli1,[21] the extracellular matrix protein tenascin C (TNC),[22] or markers for contractile pericytes.[19,23] We were interested to see which of these renal interstitial cell (RIC) populations carry PDGFR-β and if they are capable of producing EPO in response to HIF stabilization. To address these questions we used *in situ* hybridization to analyze colocalization of various markers with PDGFR-β. Moreover, we studied if cells carrying these markers are able to produce EPO under hypoxemic stimuli, targeted inhibition of HIF degradation, and pathologic conditions. With the production of EPO, renal interstitial PDGFR-β+ cells contribute to the maintenance of normal tissue oxygenation. Considering their important function as an oxygen sensor and for hormone production, the question was raised whether EPO-producing cells coexpress other functional regulatory proteins in states of hypoxia.

RESULTS

Localization and quantification of PDGFR-β-expressing cells was performed by RNAscope. On 5-μm transverse mouse kidney sections through the renal papilla, we counted an average of 6500 PDGFR-β+ RICs, which were distributed over all kidney zones (Figure 1). Approximately 50% of PDGFR-β+ RICs were located in the cortex, 40% in the OM (even distribution between outer and inner stripe) and 10% in the inner medulla (IM). In addition to interstitial cells, glomerular mesangial cells expressed PDGFR-β.

The localization and quantification of CD73 expression was analyzed by *in situ* hybridization for CD73 and PDGFR-β mRNA. CD73 expression was located in interstitial cells, glomerular mesangial cells, and proximal tubular cells, most prominently in the S3 segment. Counting the colocalization with PDGFR-β revealed that approximately 60% of all interstitial PDGFR-β+ cells coexpressed CD73. Coexpression occurred along a clear corticomedullary gradient (Figure 1, top row) and was highest in the cortex (>90% of PDGFR-β+ RICs). In the OM, coexpression only occurred in the outer zone (45% of PDGFR-β+ RICs). In the inner zone of the OM and in the IM, CD73/PDGFR-β coexpression was undetectable.

Quantification of Gli1+ (glioma-associated antigen 1) cells was investigated by immunohistochemical analysis of cells expressing green fluorescent protein (GFP) after Gli1 promoter–driven Cre recombinase activity (Gli1$^{CreERT2/+}$ mT/mG mice). This approach was necessary, as endogenous Gli1 expression levels are too low to allow for a robust quantification. Approximately 15% of all PDGFR-β+ RICs costained for Gli1-driven GFP in reporter mice, with the highest coexpression in the outer zone of the OM. In the cortex and in the inner zone of the OM, only few PDGFR-β+ cells coexpressed Gli1-driven GFP. In the IM, Gli1-driven GFP expression was almost undetectable (Figure 1, second row).

For the quantification of SMMHC expression, as a marker for contractile pericytes, immunohistochemistry was performed on reporter mice expressing GFP in all cells with Cre activity under control of the SMMHC promoter (SMMHC$^{CreERT2/+}$ mT/mG mice). SMMHC was detected in smooth muscle cells of renal vessels and in interstitial cells. Approximately 10% of all interstitial PDGFR-β+ cells coexpressed SMMHC in the OM. In the cortex and in the IM, colocalization was less than 5% (Figure 1, third row).

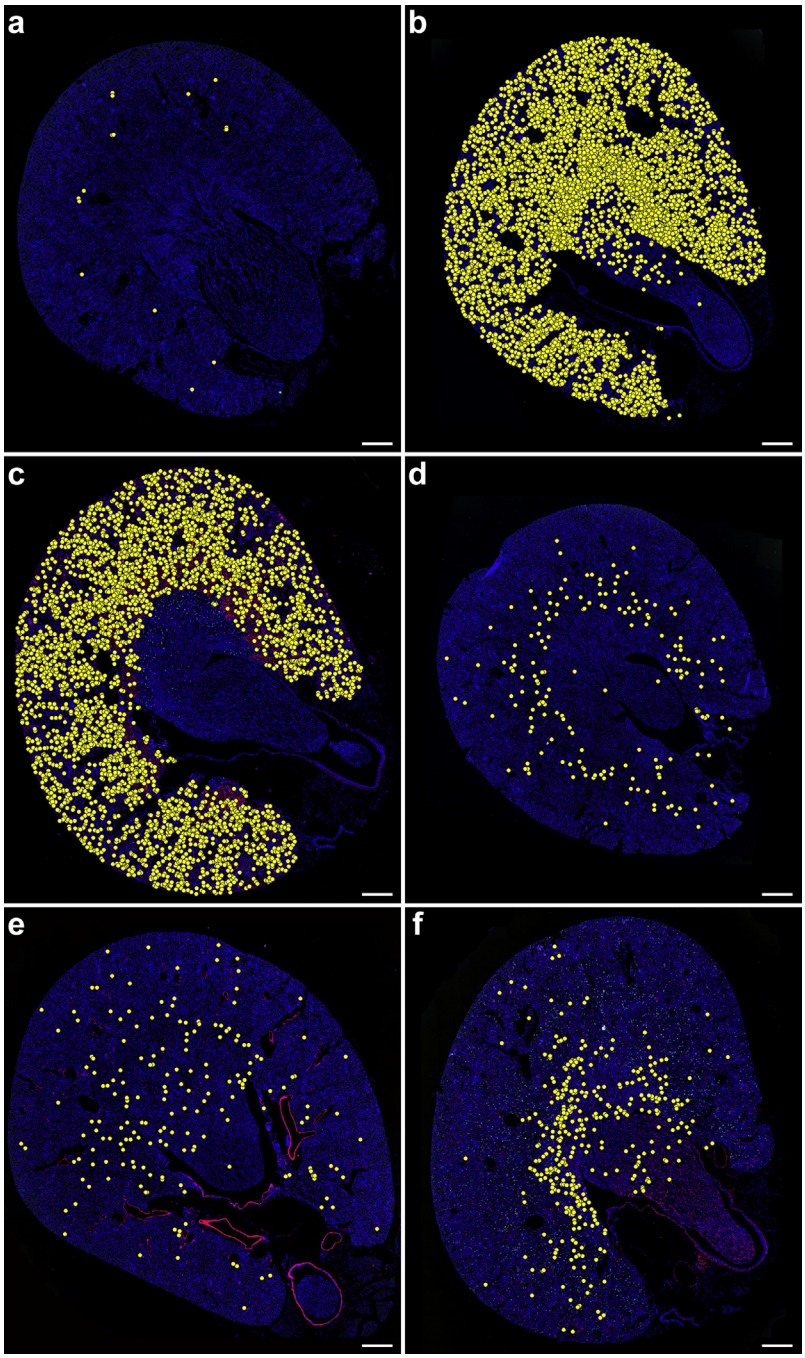

Figure 2 | Localization of cells coexpressing erythropoietin (EPO) mRNA with respective cell marker mRNA and distribution of EPO^{+} cells in the respective mouse models. Yellow dots indicate either EPO/marker coexpressing cells or distribution of EPO expressing cells, respectively. Bars = 500 μm. (**a**) Distribution of EPO expressing cells on a wild-type kidney. (**b**) Distribution of EPO expressing cells on a PDGFRβ-Vhl-KO kidney. (**c**) Localization of EPO/CD73 coexpressing cells on a PDGFRβ-Vhl-KO kidney. (**d**) Distribution of EPO expressing cells on a Gli1$^{CreERT2/+}$ Vhl$^{fl/fl}$ kidney. (**e**) Localization of EPO/SMMHC coexpressing cells on an SMMHC$^{CreERT2/+}$ Vhl$^{fl/fl}$ kidney. (**f**) Localization of EPO/tenascin C coexpressing cells on a PDGFRβ-Vhl-KO kidney. To optimize viewing of this image, please see the online version of this article at www.kidney-international.org/.

Across the kidney, approximately 25% of all PDGFR-β^{+} RICs coexpressed TNC. Coexpression of TNC by PDGFR-β^{+} cells occurred along a reverse corticomedullary gradient. Colocalization rate was low in the cortex and in the outer zone of the OM (<5%), but increased from 65% in the inner zone of the OM to 100% in the IM (Figure 1, bottom row).

Detection of either CD73^{+}, Gli1-GFP^{+}, SMMHC-GFP^{+}, or TNC^{+} interstitial cells without coexpression of PDGFR-β was very low (<3%), suggesting that these are all pure subpopulations of interstitial PDGFR-β^{+} cells.

In total, we counted on average 3900 CD73^{+}, 950 Gli1-driven GFP^{+}, 600 SMMHC^{+}, and 1600 TNC^{+} interstitial cells among

Table 2 | Hematocrit values, plasma EPO concentrations, and relative EPO mRNA expression levels in control mice, PDGFR-β$^{CreERT2/+}$ Vhl$^{fl/fl}$ mice, Gli1$^{CreERT2/+}$ Vhl$^{fl/fl}$ mice, and SMMHC$^{CreERT2/+}$ Vhl$^{fl/fl}$ mice after feeding a tamoxifen containing chow for 4 weeks

Genotype	Hematocrit values (%)	Plasma EPO concentrations (pg/ml)	EPO mRNA expression level (a.u.)
Control	49.8 ± 0.6	137.9 ± 18.8	1.0 ± 0.2
PDGFR-β$^{CreERT2/+}$ Vhl$^{fl/fl}$	71.9 ± 1.5	121,026.0 ± 13,019.0	183.1 ± 10.9
Gli1$^{CreERT2/+}$ Vhl$^{fl/fl}$	70.8 ± 0.8	1335.9 ± 95.6	20.8 ± 4.5
SMMHC$^{CreERT2/+}$ Vhl$^{fl/fl}$	69.2 ± 1.6	1278.9 ± 93.0	9.6 ± 1.5

a.u., arbitrary units; EPO, erythropoietin.
Values are the mean ± SEM of 8 mice in each group.

6500 PDGFR-β$^+$ cells on a kidney section. Table 1 gives an overview of the degree of colocalization between PDGFR-β and the respective second markers as well as the colocalization between the additional markers among each other.

Coexpression of erythropoietin mRNA with different cell markers of PDGFR-β subpopulations

On kidney sections of wild-type mice, we counted on average 10 EPO mRNA–expressing cells (Figure 2a) that were all positive for PDGFR-β and CD73. Induction of EPO expression in PDGFR-β$^+$ cells was achieved by the inducible deletion of the von Hippel-Lindau (Vhl) gene (PDGFR-β$^{CreERT2/+}$ Vhl$^{fl/fl}$, referred to as PDGFRβ-Vhl-KO), which led to the stabilization of hypoxia inducible transcription factors.[13] On kidney sections of PDGFRβ-Vhl-KO mice, we counted on average 4600 interstitial cells expressing EPO mRNA. In line with this, PDGFRβ-Vhl-KO mice were polycythemic and had increased plasma EPO levels (Table 2) after tamoxifen feeding. EPO expression was strongly induced in the cortex and the OM but only to a minor extent in the IM. Approximately 60% of EPO$^+$ RICs were located in the cortex, 35% in the OM, and less than 5% were located in the IM (Figure 2b). In addition, on average 70 mesangial cells per kidney section expressed EPO mRNA (Figure 3).

EPO and CD73 mRNA expression was localized by *in situ* hybridization on kidney sections of PDGFRβ-Vhl-KO mice. Coexpression mirrored the zonal gradient observed for the colocalization of CD73 with PDGFR-β (Figures 2c and 4a). It was highest in the cortex, here more than 95% of EPO$^+$ RICs expressed CD73. In the OM, coexpression occurred mostly in the outer zone (50% CD73$^+$ EPO cells). EPO/CD73 coexpression in the inner zone of the OM and in the IM was absent. In summary, over 75% of all EPO$^+$ RICs coexpressed CD73, suggesting an important role of interstitial CD73$^+$ cells for hypoxia-induced EPO expression.

To test for the ability of Gli1$^+$ cells to express EPO, we used mice with a conditional deletion of Vhl in Gli1$^+$ cells (Gli1$^{CreERT2/+}$ Vhl$^{fl/fl}$). After tamoxifen treatment, mice became polycythemic and had increased plasma EPO concentrations and renal EPO mRNA expression levels (Table 2). No extrarenal EPO mRNA induction was detectable. A total of 90% of EPO-expressing cells were located in the outer stripe of the OM. The cortex contained approximately 10% EPO-expressing cells (Figure 2d). All EPO$^+$ cells coexpressed PDGFR-β (Figure 4b).

In situ hybridization for EPO and SMMHC on kidney sections of PDGFRβ-Vhl-KO mice showed that approximately 5% of all EPO$^+$ RICs coexpressed SMMHC. SMMHC coexpression with EPO was mostly found in the OM (Supplementary Figure S1), where approximately 13% of EPO cells coexpressed SMMHC (Figure 4c). However, SMMHC is also strongly expressed by smooth muscle cells in the walls of arteries and arterioles. Because these cells do commonly not express PDGFR-β, hypoxia signaling in these cells was not triggered in PDGFRβ-Vhl-KO mice. To investigate the ability of SMMHC$^+$ cells to produce EPO, we

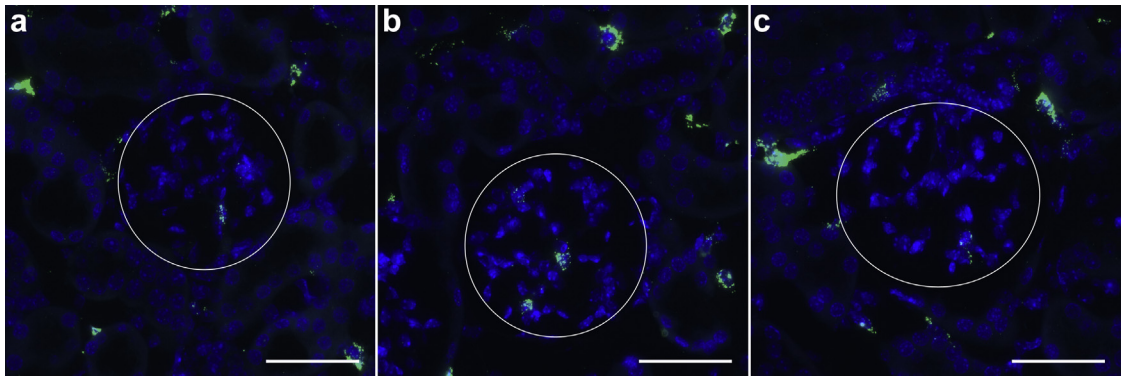

Figure 3 | Erythropoietin (EPO) mRNA expression in glomeruli, presumably mesangial cells. (**a–c**) EPO expression was found in 1–3 intraglomerular cells in approximately 35% of glomeruli (encircled) per kidney section of PDGFRβ-Vhl-KO mice. Bars = 50 μm. To optimize viewing of this image, please see the online version of this article at www.kidney-international.org/.

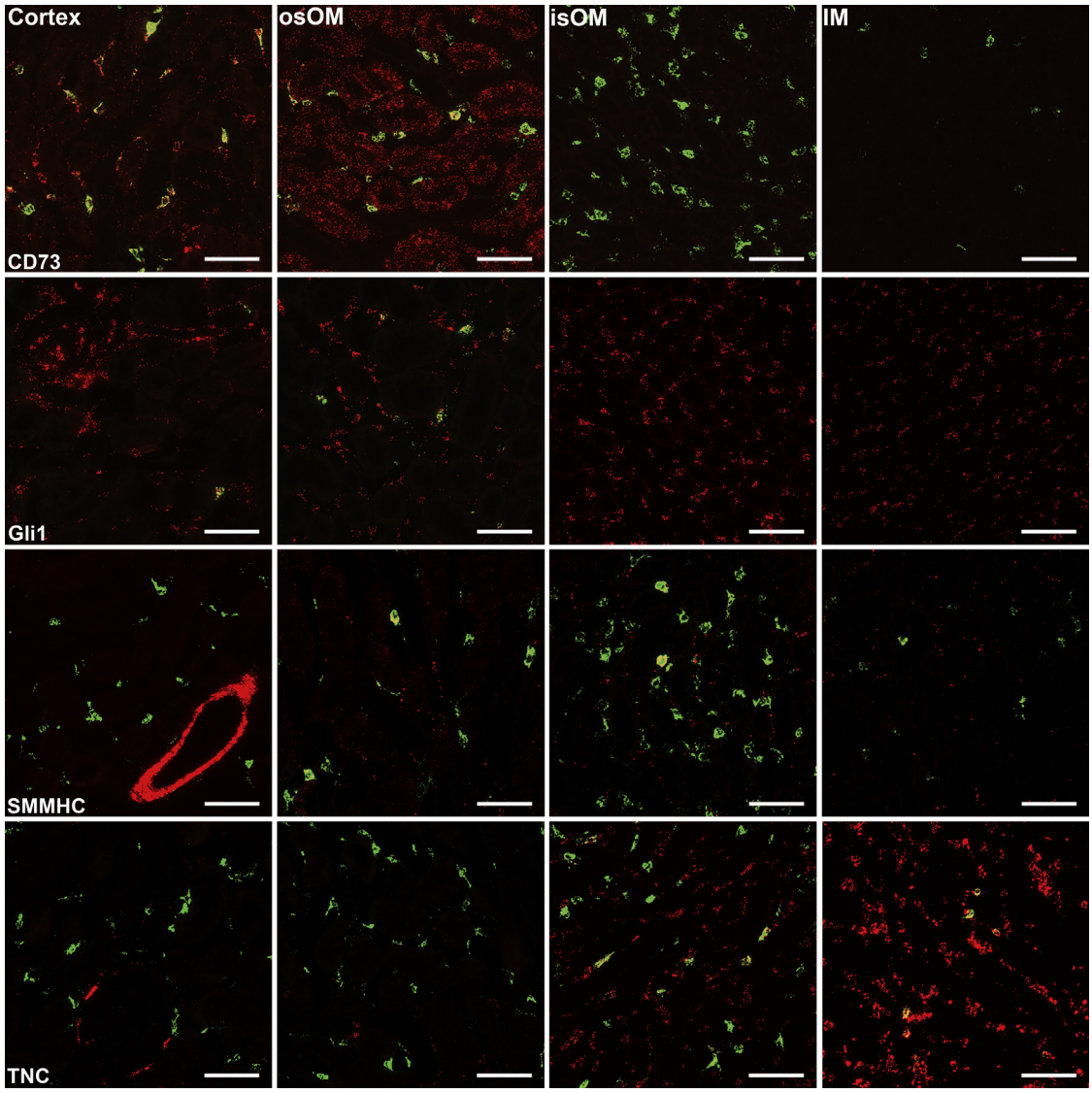

Figure 4| Cohybridization of erythropoietin (EPO) mRNA with different cell marker mRNAs in the kidney cortex, outer stripe of the OM (osOM), inner stripe of the OM (isOM), and inner medulla (IM). Yellow color results from merger of red and green fluorescence and indicates coexpression of 2 different mRNAs. Bars = 50 μm. Top row: colocalization of EPO mRNA (green) and CD73 mRNA (red) on a section of a PDGFRβ-Vhl-KO kidney. In the cortex, almost all EPO-producing cells expressed CD73; in the osOM, colocalization was approximately 50%; and in the isOM and IM, there were no EPO^{+}/CD73^{+} cells. Second row: colocalization of EPO mRNA (green) and PDGFR-β mRNA (red) on a section of a Gli1Cre$^{ERT2/+}$ Vhl$^{fl/fl}$ kidney. EPO mRNA–expressing cells were mainly found in the outer zone of the OM. All EPO mRNA–expressing cells also expressed PDGFR-β. Third row: colocalization of EPO mRNA (green) and SMMHC mRNA (red) on a section of a PDGFRβ-Vhl-KO kidney. Coexpression was highest in the OM, where approximately 15% of EPO-expressing cells coexpressed SMMHC. Bottom row: colocalization of EPO (green) and tenascin C (TNC; red) on a section of a PDGFRβ-Vhl-KO kidney. In the cortex and outer zone of the OM, no cohybridization became apparent, whereas in the inner zone of the OM, approximately 25% of EPO-expressing cells coexpressed TNC. In the IM, only a minority of TNC^{+} cells expressed EPO mRNA. To optimize viewing of this image, please see the online version of this article at www.kidney-international.org/.

generated SMMHC$^{CreERT2/+}$ Vhl$^{fl/fl}$ mice. After induction, mice were polycythemic and had increased plasma EPO concentrations and renal EPO mRNA expression levels (Table 2). No extrarenal EPO mRNA induction was found in these mice. Localization of EPO mRNA in these kidneys (Figure 2e) was similar to the colocalization of EPO and SMMHC in kidneys of PDGFRβ-Vhl-KO mice (Supplementary Figure S1). Smooth muscle cells of arteries and arterioles did not express EPO.

EPO and TNC mRNA was localized on sections of PDGFRβ-Vhl-KO mice. Coexpression of EPO and TNC was less than 5% in the cortex and in the outer zone of the OM. In the inner stripe of the OM, approximately 30% of EPO^{+} RICs coexpressed TNC. In the IM, all EPO-expressing cells colocalized with TNC (Figures 2f and 4d). However, there were a large number of TNC^{+} cells in the IM, which did not express EPO.

In total, we counted an average of 3500 CD73^{+}, 200 SMMHC^{+}, 450 TNC^{+}, and 160 Gli1-inducible EPO-

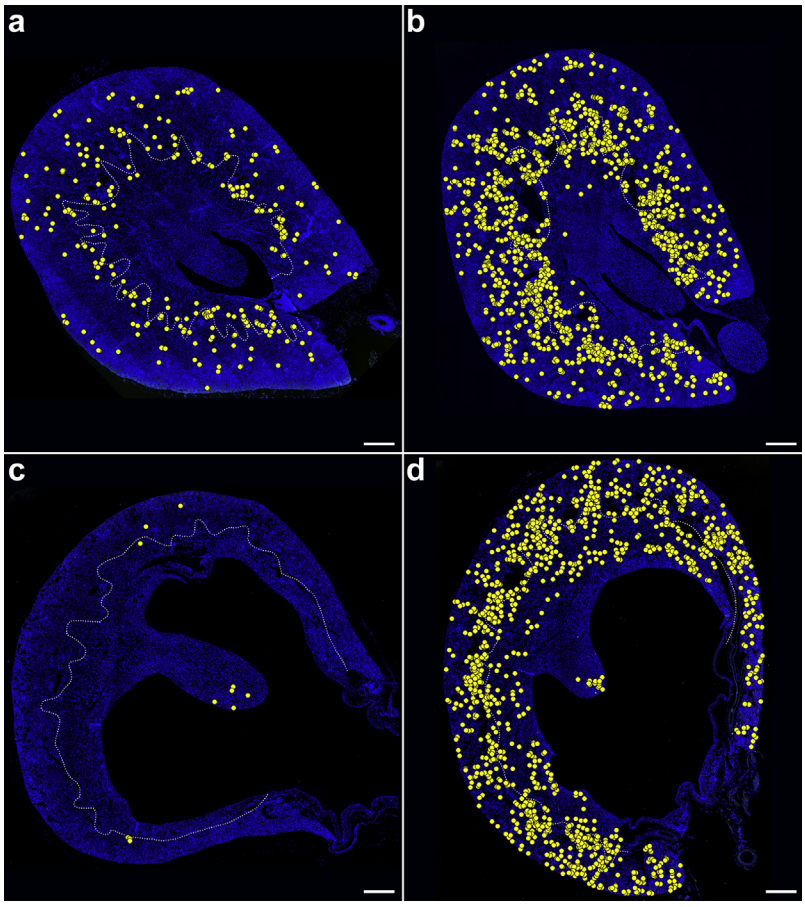

Figure 5| Localization of cells expressing erythropoietin (EPO) mRNA after 2 different hypoxic stimuli and pathologic conditions in wild-type and PDGFRβ-Vhl-KO kidneys. Yellow dots indicate EPO-producing cells. The white dotted line indicates the border between the cortex and the outer stripe of the outer medulla. Nuclei were counterstained with 4′,6-diamidino-2-phenylindole. Bars = 500 μm. (**a**) Kidney section of a wild-type mouse treated with 8% O_2 for 3 hours. Recruitment of additional EPO-expressing cells occurred mostly in the cortical region and to a minor extent (20%) in the outer stripe of the outer medulla. (**b**) Kidney section of a wild-type mouse treated with 0.1% CO for 4 hours. The number of EPO mRNA–producing cells was greatly increased mostly in the cortex. Moreover, 21% of the additional EPO-expressing cells were recruited in the outer stripe of the outer medulla. (**c**) In a 10-day unilateral ureteral obstruction (UUO) kidney of a wild-type mouse, EPO expression was reduced. Interestingly, few EPO-producing cells could be detected in the inner medulla (IM). (**d**) In a 10-day UUO kidney of a PDGFRβ-Vhl-KO mouse, a large number of EPO-expressing cells were still detectable in the cortex and the outer medulla. However, EPO production was reduced compared with a healthy PDGFRβ-Vhl-KO kidney. There were also still some EPO-producing cells in the IM. To optimize viewing of this image, please see the online version of this article at www.kidney-international.org/.

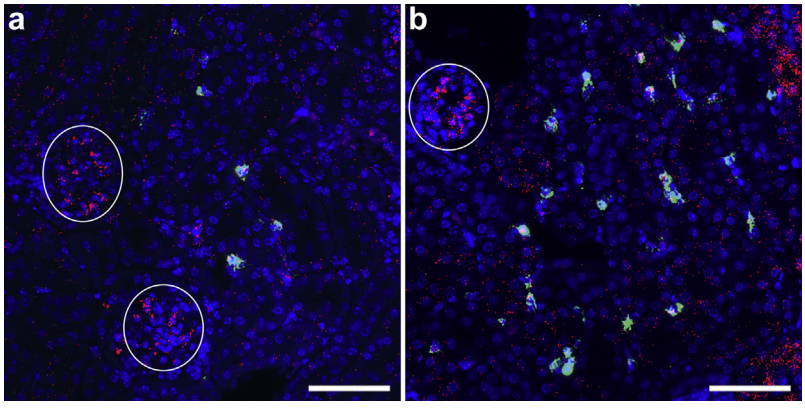

Figure 6| Double fluorescent *in situ* hybridization for erythropoietin (EPO) (green) and CD73 (red) mRNA on kidney sections of wild-type mice exposed to (a) low oxygen or (b) CO. Under both conditions, EPO-producing cells were mainly located in the cortex in a grouped fashion. The recruited EPO^+ cells were mostly part of the $CD73^+$ subpopulation. Circles indicate glomeruli. Bars = 50 μm. To optimize viewing of this image, please see the online version of this article at www.kidney-international.org/.

Table 3 | Average number of EPO-producing cells per transverse kidney section, their localization, and contributing subpopulations of PDGFR-β$^+$ interstitial cells

Treatment/genotype	Average number of EPO$^+$ cells per section	Localization of EPO$^+$ cells	Subpopulations
Untreated wild-type	10 ± 3	>99% cortex <1% osOM	CD73
8% O_2 for 3 h	242 ± 35	80% cortex 20% osOM	CD73, Gli1
0.1% CO for 4 h	1096 ± 113	78% cortex 21% osOM <1% isOM	CD73, Gli1
Wild-type UUO	8 ± 3	50% cortex 8% OM 42% IM	CD73, TNC
PDGFRβ-Vhl-KO UUO	1732 ± 114	65% cortex 34% OM <1% IM	CD73, Gli1, SMMHC, TNC

EPO, erythropoietin; IM, inner medulla; isOM, inner stripe of outer medulla; OM, outer medulla; osOM, outer stripe of outer medulla; TNC, tenascin C; UUO, unilateral ureteral obstruction.

expressing cells among the average 4600 EPO$^+$ cells on kidney sections of PDGFRβ-Vhl-KO mice (Table 1).

To evaluate the contribution of different PDGFR-β subpopulations to the EPO production in wild-type mice with nongenetic induction of the hypoxia-signaling pathway, we exposed mice to either low oxygen (8% O_2 for 3 hours) or carbon monoxide (0.1% CO for 4 hours). RNAscope for EPO mRNA on kidney sections of these mice showed a recruitment of EPO-producing cells predominantly along the corticomedullary border and in the cortex for both conditions (Figure 5a and b). Compared with normoxic conditions the number of EPO$^+$ cells increased 24-fold under low oxygen conditions and approximately 100-fold after CO exposure. The recruitment of EPO-producing cells occurred in a cluster-like fashion. These cells coexpressed CD73 (Figure 6) along with PDGFR-β. Some EPO-expressing cells were positive for Gli1, but none for SMMHC or TNC (Table 3).

In chronic kidney disease in human patients, EPO production in the kidney declines drastically.[15,16] Therefore, we induced kidney fibrosis in mice using 10 days' unilateral ureteral obstruction (UUO) to evaluate which cells are able to produce EPO under these conditions. In wild-type mice, only few cortical EPO cells were detected in the UUO kidney (Figure 5c), which belonged to the CD73 subpopulation. Interestingly, a number of EPO$^+$ cells were detectable in the remaining tissue of the IM. These atypically located EPO cells belonged to the TNC subpopulation. The UUO kidneys of PDGFRβ-Vhl-KO mice still showed a strong EPO mRNA signal in CD73$^+$ cells of the kidney cortex (Table 3). We could also detect some EPO$^+$ cells in the IM as under basal conditions. There was however only weak EPO expression in the damaged fibrotic zone of the OM (Figure 5d), where a strong induction of α-SMA mRNA could be detected by RNAscope (Supplementary Figure S2).

ADM and RGS4 coexpression with EPO

Previous data of mesangial cells with Vhl deletion showed a strong upregulation for EPO, regulator of G protein signaling 4 (RGS4), and adrenomedullin (ADM).[24] Expression of these genes was also upregulated in PDGFRβ-Vhl-KO kidneys (Table 4). With additional deletion of Hif-2α (PDGFR-β$^{CreERT2/+}$ Vhl$^{fl/fl}$ Hif-2α$^{fl/fl}$ mice), the induction of these mRNAs was almost absent, suggesting an HIF-2-regulated gene transcription similar to EPO. ADM and RGS4 mRNA abundance was increased in all zones of PDGFRβ-Vhl-KO kidneys (Figure 7). Compared with the zonal expression of EPO, which showed the highest abundance in the OM and the lowest abundance in the IM, ADM and RGS4 were more evenly distributed across the different kidney zones. We therefore analyzed cellular coexpression of EPO with ADM or RGS4 under different conditions.

Wild-type kidneys showed a weak basal expression of ADM and RGS4 in glomeruli and some PDGFR-β$^+$ RICs (Figures 8a and 9a). In addition, ADM could be detected in certain cortical tubules (Figure 8a) and RGS4 in vascular smooth muscle cells (Figure 9a). Using *in situ* hybridization

Table 4 | Relative mRNA abundance of EPO, ADM and RGS4 of control, PDGFR-β$^{CreERT2/+}$ Vhl$^{fl/fl}$, and PDGFR-β$^{CreERT2/+}$ Vhl$^{fl/fl}$ Hif-2α$^{fl/fl}$ kidneys

mRNA/RPL32mRNA (a.u.)	Control	PDGFR-β$^{CreERT2/+}$ Vhl$^{fl/fl}$	PDGFR-β$^{CreERT2/+}$ Vhl$^{fl/fl}$ Hif2α$^{fl/fl}$
EPO	1.0 ± 0.2	190.0 ± 15.0	1.5 ± 0.4
ADM	1.0 ± 0.05	4.0 ± 0.3	1.4 ± 0.2
RGS4	1.0 ± 0.1	14.0 ± 3.0	1.2 ± 0.3

ADM, adrenomedullin; EPO, erythropoietin; RGS4, regulator of G protein signaling 4.
mRNA expression levels of control mice are set to 1 and serve as a reference. Data are means ± SEM of 5 mice in each group.

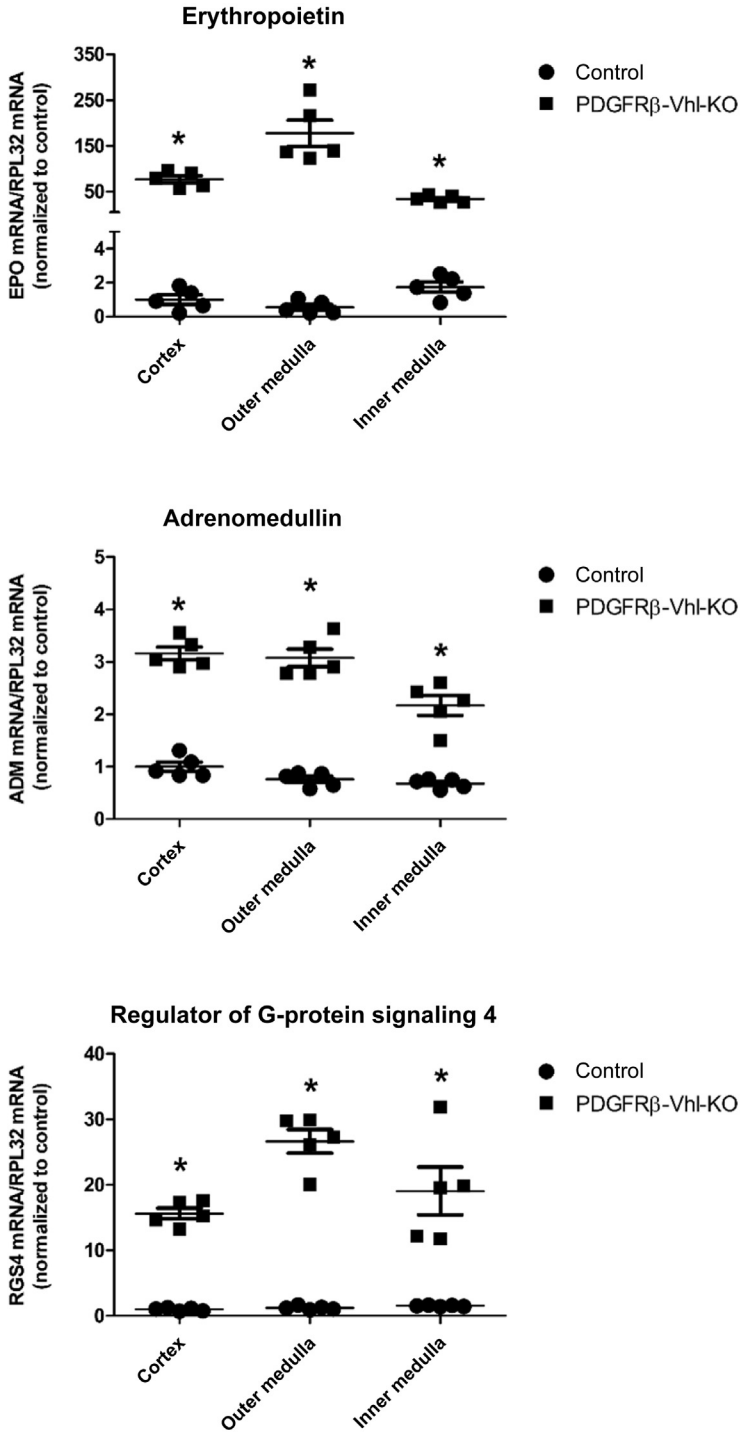

Figure 7 | Zonal mRNA expression levels of erythropoietin (EPO), adrenomedullin (ADM), and regulator of G protein signaling 4 (RGS4) in control kidneys compared with PDGFRβ-Vhl-KO kidneys. EPO, ADM, and RGS4 mRNA abundance was increased in all zones of PDGFRβ-Vhl-KO kidneys. The cortex of control kidneys is set to 1. Data are means ± SEM of 5 mice in each group. *$P < 0.05$ versus controls.

we found that all EPO$^+$ cells in wild-type kidneys coexpress ADM and RGS4 (Figures 8b and 9b). In PDGFRβ-Vhl-KO kidneys, ADM and RGS4 mRNA expression was increased in mesangial and interstitial cells of all kidney zones including the IM (Figures 8d and 9d). Interstitial ADM and RGS4 expression colocalized well with EPO expression. ADM and RGS4 also colocalized with all the markers described for EPO above (not shown). Moreover, in SMMHC$^{CreERT2/+}$ Vhl$^{fl/fl}$ and Gli1$^{CreERT2/+}$ Vhl$^{fl/fl}$ kidneys, ADM and RGS4 colocalized with EPO. Under hypoxemic conditions with low O_2 or CO treatment, we could detect a distinct upregulation of ADM and RGS4 predominantly in RICs that also started to express

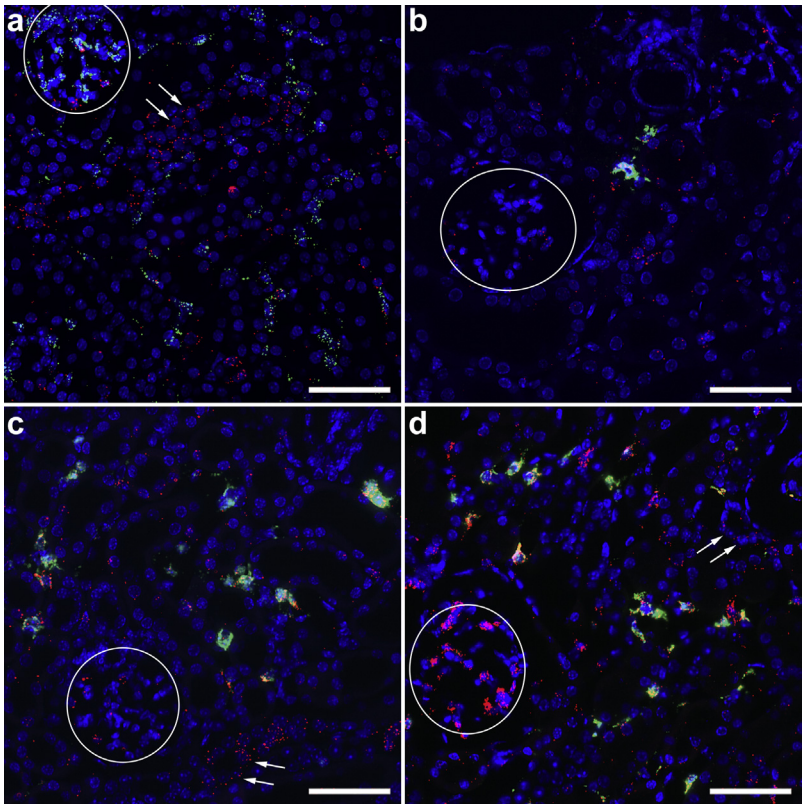

Figure 8 | Colocalization of adrenomedullin (ADM) with either PDGFR-β or erythropoietin (EPO). Circles indicate glomeruli. Bars = 50 μm. (**a**) RNAscope for ADM (red) and PDGFR-β (green) in the cortex of a wild-type kidney. Weak ADM expression was detected in glomerular mesangial cells, some interstitial PDGFR-β$^+$ cells, and certain tubular segments (arrows). (**b**) RNAscope for ADM (red) and EPO (green) on a wild-type kidney. All native EPO-expressing renal interstitial cells (RICs) also express ADM. (**c**) ADM (red) and EPO (green) expression on a kidney section of a wild-type mouse exposed to 8% O_2 for 3 hours. ADM was upregulated in all recruited EPO cells. Tubular ADM expression was not affected by low oxygen treatment (arrows). (**d**) In PDGFRβ-Vhl-KO kidneys, ADM (red) was strongly upregulated in all cells affected by the deletion of Vhl, namely glomerular mesangial cells and RICs. All EPO (green)-expressing cells of PDGFRβ-Vhl-KO mice showed a strong upregulation of ADM. To optimize viewing of this image, please see the online version of this article at www.kidney-international.org/.

EPO (Figures 8c and 9c). UUO had no effect on the interstitial ADM and RGS4 mRNA expression of the kidney.

DISCUSSION

On the basis of our findings that renal cells capable of producing EPO carry the PDGFR-β,[13] this study aimed to further characterize potential renal EPO-producing cells. We found EPO mRNA–expressing cells in the interstitium of the cortex, the OM, and less in the IM after inducible deletion of Vhl in PDGFR-β$^+$ cells.[13] This broad interzonal distribution of potential EPO-expressing cells is not specific for the deletion of Vhl but can also be produced by deletion of HIF prolyl-4-hydroxylase 2 in the FoxD1 cell lineage[9] and by severe anemia.[2]

In accordance with previous reports, we identified subpopulations of PDGFR-β$^+$ cells, which expressed CD73, Gli1, SMMHC, and TNC.[21,22,25] PDGFR-β$^+$/CD73$^+$ RICs were located in the cortex, including the border between the cortex and the OM. PDGFR-β$^+$/Gli1$^+$ RICs were predominantly found in the outer zone of the OM. PDGFR-β$^+$/SMMHC$^+$ cells were mainly detected in the OM. PDGFR-β$^+$/TNC$^+$ cells were located in the IM and in the inner zone of the OM. Again, these results are in good accordance with previous reports.[21,22,26] After inducible deletion of Vhl from PDGFR-β$^+$ cells, we found EPO expression in nearly all interstitial CD73$^+$ cells, which made up approximately 65% of all PDGFR-β$^+$ EPO-expressing cells. This observation supports previous reports identifying nontubular CD73$^+$ cells as the quantitative dominant intrarenal site of physiologic EPO production.[1,2] The remaining 35% of EPO-expressing PDGFR-β$^+$ cells were mostly localized in the OM, where CD73$^+$, Gli1$^+$, TNC$^+$, and interstitial SMMHC$^+$ cells were found.[21,22,27] The cell-specific deletion of Vhl in Gli1$^+$ cells induced EPO expression and caused polycythemia. These results are supported by a recent study suggesting Gli1$^+$ cells as possible production sites for EPO.[28] EPO-expressing cells showed the characteristic stellate appearance described for EPO-expressing cells of anemic kidneys[10,14] or of PDGFR-β$^{CreERT2/+}$ Vhl$^{fl/fl}$ mice[13] (Supplementary Figure S3). Gli1$^+$ cells are considered closely related to pericytes, which transform into myofibroblasts in states of interstitial kidney fibrosis.[29,30]

In addition, cells expressing SMMHC appear as potential EPO producers. Apparently, only interstitial SMMHC$^+$ cells,

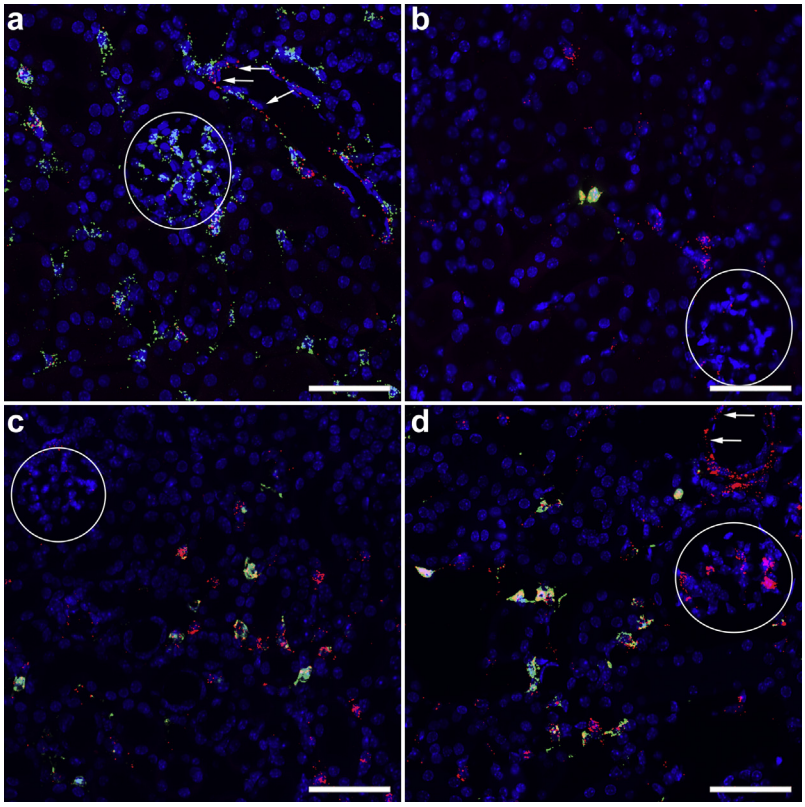

Figure 9 | Colocalization of regulator of G protein signaling 4 (RGS4) with either PDGFR-β or erythropoietin (EPO). Circles indicate glomeruli. Bars = 50 μm. (**a**) RNAscope for RGS4 (red) and PDGFR-β (green) on a wild-type kidney. In the cortical region, weak RGS4 expression was detected in some glomerular mesangial cells, interstitial PDGFR-β$^+$ cells, and renal vessels. (**b**) RNAscope for RGS4 (red) and EPO (green) under basal conditions. All native EPO-expressing renal interstitial cells (RICs) also expressed RGS4. (**c**) RGS4 (red) and EPO (green) expression on a kidney section of a wild-type mouse exposed to 8% O_2 for 3 hours. RGS4 was expressed similar to adrenomedullin in all EPO-producing cells and in RICs close to EPO cells. (**d**) In PDGFRβ-Vhl-KO kidneys, RGS4 (red) was strongly upregulated in all cells affected by the deletion of Vhl, glomerular mesangial cells, and RICs. All EPO (green)-expressing cells of PDGFRβ-Vhl-KO mice showed a strong upregulation of RGS4. To optimize viewing of this image, please see the online version of this article at www.kidney-international.org/.

but not vascular smooth muscle cells in the preglomerular arteries and arterioles, could express EPO after deletion of Vhl. We therefore consider SMMHC$^+$ RICs able to express EPO as contractile pericytes.[31] These cells are known to play a role in the regulation of medullary blood flow.[31,32] In addition to CD73$^+$, Gli1$^+$, and SMMHC$^+$ RICs, a subset of medullary TNC$^+$ RICs appear to have the potential for EPO production.

To analyze the contribution of these subpopulations to the EPO-producing cells under hypoxemic conditions, we exposed mice to either low O_2 or CO. Recruitment of EPO cells occurred cluster-like along the corticomedullary border and spread throughout the kidney cortex, as described previously (Figure 5a and b).[4,7,33] The majority of the recruited EPO cells could be assigned to the CD73$^+$ subpopulation of PDGFR-β$^+$ interstitial cells (Figure 6). In the outer stripe of the OM, Gli1$^+$ cells also contributed to the additional EPO production, whereas the SMMHC and TNC subpopulations did not play a role under these conditions. These results are in good accordance with previous findings.[1,8,28]

Interestingly, the TNC$^+$ RICs identified in this study seem to play a role during experimental kidney fibrosis. During UUO this subpopulation of potential EPO-producing cells sustained a *de novo* expression of EPO mRNA in the IM whereas EPO production in the kidney cortex declined (Figure 5c). This is noteworthy because under basal conditions EPO expression could not be detected in the IM of wild-type mice. The kidneys of PDGFRβ-Vhl-KO mice retained a strong cortical EPO mRNA expression during UUO, but cells in the high fibrotic zone in the OM lost the ability to express EPO whereas they started to express α-SMA (Supplementary Figure S2).[12,14,17,34] Sporadically, EPO$^+$ cells could be detected that expressed α-SMA mRNA at the same time, but the EPO signal was already weaker in these cells compared with α-SMA$^-$ EPO cells.[7] In the IM of these mice, also a number of TNC$^+$ EPO-producing cells could still be detected (Figure 5d). These findings suggest that the TNC$^+$ subpopulation has the potential of producing EPO in this model of kidney fibrosis. This could eventually

Table 5 | Primer sequences used for genotyping

Genotype	Sequence (5′–3′), fwd	Sequence (5′–3′), rev
PDGFR-β^{CreERT2}	gaactgtcaccggcagga	aggcaaattttggtgtacgg
Vhl	ctaggcaccgagcttagaggtttgcg	ctgacttccactgatgcttgtcacag
HIF-2α	gagagcagcttctcctggaa	tgtaggcaaggaaaccaagg
Gli1^{CreERT2}	cagaacctgaagatgttc	ccagattacgtatatcc
SM-MHC^{CreERT2}	tgaccccatctcttcactcc	agtccctcacatcctcaggtt
mT/mG	ctctgctgcctcctggcttct	tcaatgggcgggggtcgtt

be used as a new target for further investigations and pharmaceutical development.

In this study, novel insights into the expression pattern of 2 factors influencing the local tissue oxygenation could be obtained. On one hand, we could show that ADM and RGS4 are coexpressed in EPO-producing cells under basal conditions (Figures 8b and 9b). On the other hand, we could detect that ADM and RGS4 were significantly coinduced in all EPO$^+$ cells after Vhl deletion in PDGFR-β$^+$ cells of the kidney as well as under hypoxemic conditions (Figures 8 and 9). These results are in good accordance with other studies showing the hypoxia inducibility of ADM and RGS4.[35–39] ADM has been described to increase renal perfusion as well as salt and water excretion.[40,41] Therefore, it is conceivable that hypoxemic induction of ADM production in the interstitium leads to an increase in interstitial perfusion and to a lowering of energy consuming sodium resorption. Both mechanisms could contribute to improving the interstitial oxygenation in states of hypoxia. Similarly, RGS4 expression in perivascular PDGFR-β$^+$ cells could contribute to counteracting or attenuating vasoconstrictor effects of mediators acting via Gq proteins. Some evidence for such a vascular and renoprotective effect of RGS4 has already been provided.[42–44]

Taken together, it is conceivable that PDGFR-β$^+$ RICs play an important role as an oxygen-sensing system that helps the kidney to improve tissue oxygenation in states of hypoxia. It is noteworthy in this context that in the normal kidney EPO, ADM, and RGS4 mRNA levels are very low in interstitial PDGFR-β$^+$ cells but substantially increase after induction of HIF signaling. Moreover, we want to highlight that the PDGFR-β$^+$ RICs can be subdivided into different subpopulations, which are in principle able to produce EPO. Depending on the stimulus, different subpopulations are recruited to express EPO. Under hypoxemic conditions, CD73$^+$ and Gli1$^+$ cells predominantly contribute to EPO production, whereas under profibrotic pathologic situations, TNC$^+$ RICs seem to be activated. Because of the wide intrarenal distribution and high number of potential EPO/ADM/RGS4-producing PDGFR-β$^+$ RICs, this cell pool will form a target for newly developed drugs such as HIF prolyl-4-hydroxylase-inhibitors, which not only stimulate EPO production but could also ameliorate progression of renal disease.[45–47]

Table 6 | RNAscope probes[a] used for *in situ* hybridization

RNAscope probe	Cat no.
Mm-Adm	493601
Mm-Epo-C2	315501-C2
Mm-Myh11 (SMMHC)	316101
Mm-Nt5e (CD73)	437951
Mm-Pdgfrb-C2	411381-C2
Mm-Rgs4	467461
Mm-Tnc	465021
Mm-Acta2	319531
2.5 Duplex Positive Control Probe -Mm	321651
2-plex Negative Control Probe	320751
Positive Control Probe- Mm-Ppib	313911
Negative Control Probe-DapB	310043

[a]Advanced Cell Diagnostics, Newark, CA.

Table 7 | Primer sequences used for qPCR

Genes	Sequence (5′–3′)	Product size (bp)
RPL32	fwd: ttaagcgaaactggcggaaac rev: ttgttgctcccataaccgatg	100
ADM	fwd: gactcgctgatgagacgaca rev: gaaccctggttcatgctctg	145
EPO	fwd: aatggaggtggaagaacagg rev: acccgaagcagtgaagtga	174
RGS4	fwd: aatagaaaccaccgcggctc rev: gaaagctgccagtccacatt	292

ADM, adrenomedullin; EPO, erythropoietin; RGS4, regulator of G protein signaling 4; RPL32, ribosomal protein L32.

MATERIALS AND METHODS

Animals

PDGFR-β$^{CreERT2/+}$ Vhl$^{fl/fl}$ and PDGFR-β$^{CreERT2/+}$ Vhl$^{fl/fl}$ HIF-2α$^{fl/fl}$ mice were generated by crossbreeding PDGFR-β^{CreERT2} mice (tamoxifen-inducible Cre recombinase expression under the control of the PDGFR-β promoter; JAX stock #029684)[24] and mice with loxP-flanked Vhl alleles[48] or additionally with mice with loxP-flanked HIF-2α alleles.[49] Gli1Cre$^{ERT2/+}$ Vhl$^{fl/fl}$ and SMMHC$^{CreERT2/+}$ Vhl$^{fl/fl}$ mice were generated by crossbreeding Gli1^{CreERT2} mice (tamoxifen-inducible Cre recombinase under the control of the Gli1 gene promotor; JAX stock #007913),[50] or SMMHC^{CreERT2} mice (tamoxifen-inducible Cre recombinase under the control of the SMMHC gene promotor; JAX stock #19079)[51] and Vhl$^{fl/fl}$ mice. For Gli1 and SMMHC lineage tracing, Gli1^{CreERT2} mice and SMMHC^{CreERT2} mice were crossed with the membrane-Tomato/membrane-GFP (mT/mG; JAX stock #007676)[52] reporter mouse strain (Gli1$^{CreERT2/+}$ mT/mG and SMMHC$^{CreERT2/+}$ mT/mG). Genotyping was performed using the primers listed in Table 5.

Animals were maintained on standard rodent chow (0.6% NaCl; Ssniff, Soest, Germany) with free access to tap water. All animal experiments were performed according to the Guidelines for the Care and Use of Laboratory Animals published by the US National Institutes of Health and approved by the local ethics committee.

Tamoxifen treatment

Cre-mediated recombination was induced by feeding a diet containing 400-mg tamoxifen citrate per kilogram (A115T00404; Ssniff) for 4 weeks followed by a 3-week period with standard chow.

Unilateral ureteral obstruction

Under inhalation anesthesia, a unilateral ureteral ligation was placed close to the kidney through an abdominal incision. Mice were kept under close observation after the operation. Ten days after the procedure mice were perfused with 10% neutral buffered formalin solution.

Low oxygen and CO exposure

To induce EPO production in kidneys of wild-type mice, these were placed either for 3 hours in a chamber containing only 8% O_2 or for 4 hours in a 0.1% CO atmosphere as described previously.[10] Animals were killed immediately at the end of the experiment for histologic analysis.

In situ hybridization via RNAscope

Localization of target mRNA was studied by using the RNAscope Multiplex Fluorescent v2 kit (Advanced Cell Diagnostics, Newark, CA), according to the manufacturer's instructions.[53] Hybridization signals were detected on 5-µm formalin-fixed paraffin-embedded transverse kidney sections using the TSA Plus fluorophores Cy3 and Cy5 (PerkinElmer, Waltham, MA). Slices were mounted with ProLong Gold Antifade Mountant (Thermo Fisher Scientific, Waltham, MA) and viewed with an Axio Observer.Z1 Microscope (Zeiss, Jena, Germany). To ensure interpretable results, positive and negative controls were routinely included. RNAscope probes used are listed in Table 6.

Immunohistochemistry

Five-micrometer sections of formalin-fixed paraffin-embedded kidneys were blocked with 10% horse serum/1% bovine serum albumin in phosphate-buffered saline and incubated with chicken anti-GFP (ab13970; Abcam, Cambridge, UK) and rabbit anti-PDGFR-β (ab32570; Abcam) or rabbit anti-SMMHC (ab53219; Abcam) antibodies at 4 °C overnight. After washing with bovine serum albumin/phosphate-buffered saline, sections were stained with Cy2 and Tritc secondary antibodies (Dianova, Hamburg, Germany), mounted with Glycergel (Agilent, Waldbronn, Germany), and viewed with an Axio Observer.Z1 Microscope.

Cell counting

Cell counting was performed using ImageJ software. Kidneys of 3 mice per genotype were analyzed for each colocalization study. Cells were counted on 3 different sections per kidney by manually placing a marker (plugin "cell counter notice"). Counting was performed by 2 persons independently in a blinded fashion.

Determination of mRNA expression by real-time polymerase chain reaction

Total RNA was isolated from kidneys as described by Chomczynski and Sacchi[54] and quantified by a photometer. One microgram of the resulting RNA was used for reverse transcription. cDNA was synthesized by Moloney murine leukemia virus RT (Thermo Fisher Scientific). For the quantification of mRNA expression, real-time polymerase chain reaction was performed using a Light Cycler Instrument and the LightCycler 480 SYBR Green I Master Kit (Roche Diagnostics, Mannheim, Germany). mRNA expression data were normalized to ribosomal protein L32. Table 7 lists primer sequences.

Determination of hematocrit values and plasma EPO concentrations

Blood samples were taken from tail vein into ethylenediamine tetraacetic acid–coated capillary tubes. Hematocrit values were determined after centrifugation (4 minutes, 12,000 rpm, room temperature). EPO protein concentration was determined in plasma samples using the Quantikine Mouse EPO ELISA kit (BioTechne, Minneapolis, MN), according to the manufacturer's protocol.

Statistical analyses

All data are presented as means ± SEM. Statistical significance was determined by Student's t test. $P < 0.05$ was considered statistically significant. Data were analyzed using Prism 5 (GraphPad Software, San Diego, CA).

DISCLOSURE

All the authors declared no competing interests.

ACKNOWLEDGMENTS

We thank Prof. Stefan Offermanns (Centre for Molecular Medicine, Medical Faculty, Goethe University, Frankfurt am Main) for providing the SMMHC$^{CreERT2/+}$ mouse line. The expert technical assistance provided by Susanne Fink, Ramona Steppan, and Svende Pfundstein is gratefully acknowledged. This work was supported by grants from the German Research Foundation (DFG; Ku 859/15-2 and SFB 1350, project number 387509280) and the Swiss National Science Foundation (National Centre of Competence in Research "Kidney.CH").

SUPPLEMENTARY MATERIAL

Supplementary File (PDF)

Figure S1. Localization of cells coexpressing EPO and SMMHC mRNA on a PDGFRβ-Vhl-KO kidney.

Figure S2. Details of the outer medulla of a double *in situ* hybridization for EPO and α-SMA mRNA on a UUO kidney section of a PDGFRβ-Vhl-KO mouse.

Figure S3. Chromogenic RNAscope for EPO mRNA on kidney sections of Gli1$^{CreERT2/+}$ Vhl$^{fl/fl}$ mice in detail.

REFERENCES

1. Bachmann S, Le Hir M, Eckardt KU. Co-localization of erythropoietin mRNA and ecto-5′-nucleotidase immunoreactivity in peritubular cells of rat renal cortex indicates that fibroblasts produce erythropoietin. *J Histochem Cytochem*. 1993;41:335–341.
2. Maxwell PH, Osmond MK, Pugh CW, et al. Identification of the renal erythropoietin-producing cells using transgenic mice. *Kidney Int*. 1993;44:1149–1162.
3. Paliege A, Rosenberger C, Bondke A, et al. Hypoxia-inducible factor-2α-expressing interstitial fibroblasts are the only renal cells that express erythropoietin under hypoxia-inducible factor stabilization. *Kidney Int*. 2010;77:312–318.
4. Eckardt K-U, Koury ST, Tan CC, et al. Distribution of erythropoietin producing cells in rat kidneys during hypoxic hypoxia. *Kidney Int*. 1993;43:815–823.
5. Koury ST, Bondurant MC, Semenza GL, Koury MJ. The use of *in situ* hybridization to study erythropoietin gene expression in murine kidney and liver. *Microsc Res Tech*. 1993;25:29–39.
6. Yamazaki S, Souma T, Hirano I, et al. A mouse model of adult-onset anaemia due to erythropoietin deficiency. *Nat Commun*. 2013;4:1950.
7. Maxwell PH, Ferguson DJP, Nicholls LG, et al. Sites of erythropoietin production. *Kidney Int*. 1997;51:393–401.
8. Pan X, Suzuki N, Hirano I, et al. Isolation and characterization of renal erythropoietin-producing cells from genetically produced anemia mice. *PLoS One*. 2011;6:e25839.
9. Kobayashi H, Liu Q, Binns TC, et al. Distinct subpopulations of FOXD1 stroma-derived cells regulate renal erythropoietin. *J Clin Invest*. 2016;126:1926–1938.
10. Imeri F, Nolan KA, Bapst AM, et al. Generation of renal Epo-producing cell lines by conditional gene tagging reveals rapid HIF-2 driven Epo kinetics, cell autonomous feedback regulation, and a telocyte phenotype. *Kidney Int*. 2019;95:375–387.
11. Kramann R, Humphreys BD. Kidney pericytes: roles in regeneration and fibrosis. *Semin Nephrol*. 2014;34:374–383.
12. Souma T, Nezu M, Nakano D, et al. Erythropoietin synthesis in renal myofibroblasts is restored by activation of hypoxia signaling. *J Am Soc Nephrol*. 2016;27:428–438.

13. Gerl K, Nolan KA, Karger C, et al. Erythropoietin production by PDGFR-β+ cells. *Pflugers Arch*. 2016;468:1479–1487.
14. Souma T, Yamazaki S, Moriguchi T, et al. Plasticity of renal erythropoietin-producing cells governs fibrosis. *J Am Soc Nephrol*. 2013;24:1599–1616.
15. Eschbach JW, Adamson JW. Anemia of end-stage renal disease (ESRD). *Kidney Int*. 1985;28:1–5.
16. Babitt JL, Lin HY. Mechanisms of anemia in CKD. *J Am Soc Nephrol*. 2012;23:1631–1634.
17. Maxwell PH, Ferguson DJP, Nicholls LG, et al. The interstitial response to renal injury: fibroblast-like cells show phenotypic changes and have reduced potential for erythropoietin gene expression. *Kidney Int*. 1997;52:715–724.
18. Lemley KV, Kriz W. Anatomy of the renal interstitium. *Kidney Int*. 1991;39:370–381.
19. Armulik A, Genové G, Betsholtz C. Pericytes: developmental, physiological, and pathological perspectives, problems, and promises. *Dev Cell*. 2011;21:193–215.
20. Urrutia AA, Afzal A, Nelson J, et al. Prolyl-4-hydroxylase 2 and 3 coregulate murine erythropoietin in brain pericytes. *Blood*. 2016;128:2550–2560.
21. Kramann R, Wongboonsin J, Chang-Panesso M, et al. Gli1+ pericyte loss induces capillary rarefaction and proximal tubular injury. *J Am Soc Nephrol*. 2017;28:776–784.
22. He W, Xie Q, Wang Y, et al. Generation of a tenascin-C-CreER2 knockin mouse line for conditional DNA recombination in renal medullary interstitial cells. *PLoS One*. 2013;8:79839.
23. Bergers G, Song S. The role of pericytes in blood-vessel formation and maintenance. *Neuro Oncol*. 2005;7:452–464.
24. Gerl K, Miquerol L, Todorov VT, et al. Inducible glomerular erythropoietin production in the adult kidney. *Kidney Int*. 2015;88:1345–1355.
25. Sato Y, Yanagita M. Resident fibroblasts in the kidney: a major driver of fibrosis and inflammation. *Inflamm Regen*. 2017;37:17.
26. Le Hir M, Eckardt KU, Kaissling B. Anemia induces 5′-nucleotidase in fibroblasts of cortical labyrinth of rat kidney. *Ren Physiol Biochem*. 1989;12:313–319.
27. Stefanska A, Eng D, Kaverina N, et al. Interstitial pericytes decrease in aged mouse kidneys. *Aging*. 2015;7:370–382.
28. Greenwald AC, Licht T, Kumar S, et al. VEGF expands erythropoiesis via hypoxia-independent induction of erythropoietin in noncanonical perivascular stromal cells. *J Exp Med*. 2019;216:215–230.
29. Kramann R, Schneider RK, DiRocco DP, et al. Perivascular Gli1+ progenitors are key contributors to injury-induced organ fibrosis. *Cell Stem Cell*. 2015;16:51–66.
30. Kramann R, Fleig SV, Schneider RK, et al. Pharmacological GLI2 inhibition prevents myofibroblast cell-cycle progression and reduces kidney fibrosis. *J Clin Invest*. 2015;125:2935–2951.
31. Park F, Mattson DL, Roberts LA, Cowley AW. Evidence for the presence of smooth muscle alpha-actin within pericytes of the renal medulla. *Am J Physiol*. 1997;273(Pt 2):R1742–R1748.
32. Pallone TL, Silldorff EP. Pericyte regulation of renal medullary blood flow. *Exp Nephrol*. 2001;9:165–170.
33. Koury ST, Koury MJ, Bondurant MC, et al. Quantitation of erythropoietin-producing cells in kidneys of mice by *in situ* hybridization: correlation with hematocrit, renal erythropoietin mRNA, and serum erythropoietin concentration. *Blood*. 1989;74:645–651.
34. Asada N, Takase M, Nakamura J, et al. Dysfunction of fibroblasts of extrarenal origin underlies renal fibrosis and renal anemia in mice. *J Clin Invest*. 2011;121:3981–3990.
35. Sandner P, Hofbauer KH, Tinel H, et al. Expression of adrenomedullin in hypoxic and ischemic rat kidneys and human kidneys with arterial stenosis. *Am J Physiol Regul Integr Comp Physiol*. 2004;286:R942–R951.
36. Nagata D, Hirata Y, Suzuki E, et al. Hypoxia-induced adrenomedullin production in the kidney. *Kidney Int*. 1999;55:1259–1267.
37. Olechnowicz SWZ, Fedele AO, Peet DJ. Hypoxic induction of the regulator of G-protein signalling 4 gene is mediated by the hypoxia-inducible factor pathway. *PLoS One*. 2012;7:e44564.
38. Zhu Q, Hu J, Han W-Q, et al. Silencing of HIF prolyl-hydroxylase 2 gene in the renal medulla attenuates salt-sensitive hypertension in Dahl S rats. *Am J Hypertens*. 2014;27:107–113.
39. Li N. Hypoxia inducible factor-1α-mediated gene activation in the regulation of renal medullary function and salt sensitivity of blood pressure. *Am J Cardiovasc Dis*. 2012;2:208–215.
40. Ebara T, Miura K, Okumura M, et al. Effect of adrnomedullin on renal hemodynamics and functions in dogs. *Eur J Pharmacol*. 1994;263:69–73.
41. Vari RC, Adkins SD, Samson WK. Renal effects of adrenomedullin in the rat. *Proc Soc Exp Biol Med*. 1996;211:178–183.
42. Siedlecki A, Anderson JR, Jin X, et al. RGS4 controls renal blood flow and inhibits cyclosporine-mediated nephrotoxicity. *Am J Transplant*. 2010;10:231–241.
43. Pang P, Jin X, Proctor BM, et al. RGS4 inhibits angiotensin II signaling and macrophage localization during renal reperfusion injury independent of vasospasm. *Kidney Int*. 2015;87:771–783.
44. Siedlecki AM, Jin X, Thomas W, et al. RGS4, a GTPase activator, improves renal function in ischemia-reperfusion injury. *Kidney Int*. 2011;80:263–271.
45. Joharapurkar AA, Pandya VB, Patel VJ, et al. Prolyl hydroxylase inhibitors: a breakthrough in the therapy of anemia associated with chronic diseases. *J Med Chem*. 2018;61:6964–6982.
46. Sakashita M, Tanaka T, Nangaku M. Hypoxia-inducible factor-prolyl hydroxylase domain inhibitors to treat anemia in chronic kidney disease. *Contrib Nephrol*. 2019;198:112–123.
47. Ogoshi Y, Matsui T, Mitani I, et al. Discovery of JTZ-951: a HIF prolyl hydroxylase inhibitor for the treatment of renal anemia. *ACS Med Chem Lett*. 2017;8:1320–1325.
48. Haase VH, Glickman JN, Socolovsky M, Jaenisch R. Vascular tumors in livers with targeted inactivation of the von Hippel-Lindau tumor suppressor. *Proc Natl Acad Sci U S A*. 2001;98:1583–1588.
49. Gruber M, Hu C-J, Johnson RS, et al. Acute postnatal ablation of Hif-2alpha results in anemia. *Proc Natl Acad Sci U S A*. 2007;104:2301–2306.
50. Ahn S, Joyner AL. Dynamic changes in the response of cells to positive hedgehog signaling during mouse limb patterning. *Cell*. 2004;118:505–516.
51. Wirth A, Benyó Z, Lukasova M, et al. G12-G13-LARG-mediated signaling in vascular smooth muscle is required for salt-induced hypertension. *Nat Med*. 2008;14:64–68.
52. Muzumdar MD, Tasic B, Miyamichi K, et al. A global double-fluorescent Cre reporter mouse. *Genes*. 2007;45:593–605.
53. Wang F, Flanagan J, Su N, et al. RNAscope: a novel in situ RNA analysis platform for formalin-fixed, paraffin-embedded tissues. *J Mol Diagn JMD*. 2012;14:22–29.
54. Chomczynski P, Sacchi N. Single-step method of RNA isolation by acid guanidinium thiocyanate-phenol-chloroform extraction. *Anal Biochem*. 1987;162:156–159.

Supplementary Material

Supplementary Figure S1: Localization of cells coexpressing EPO and SMMHC mRNA on a PDGFRβ-Vhl-KO kidney highlighted with yellow dots. Distribution of EPO/SMMHC expressing cells is similar to the distribution of EPO producing cells in kidneys of $SMMHC^{CreERT2/+}$ $Vhl^{fl/fl}$ mice. Scale bars = 500 µm.

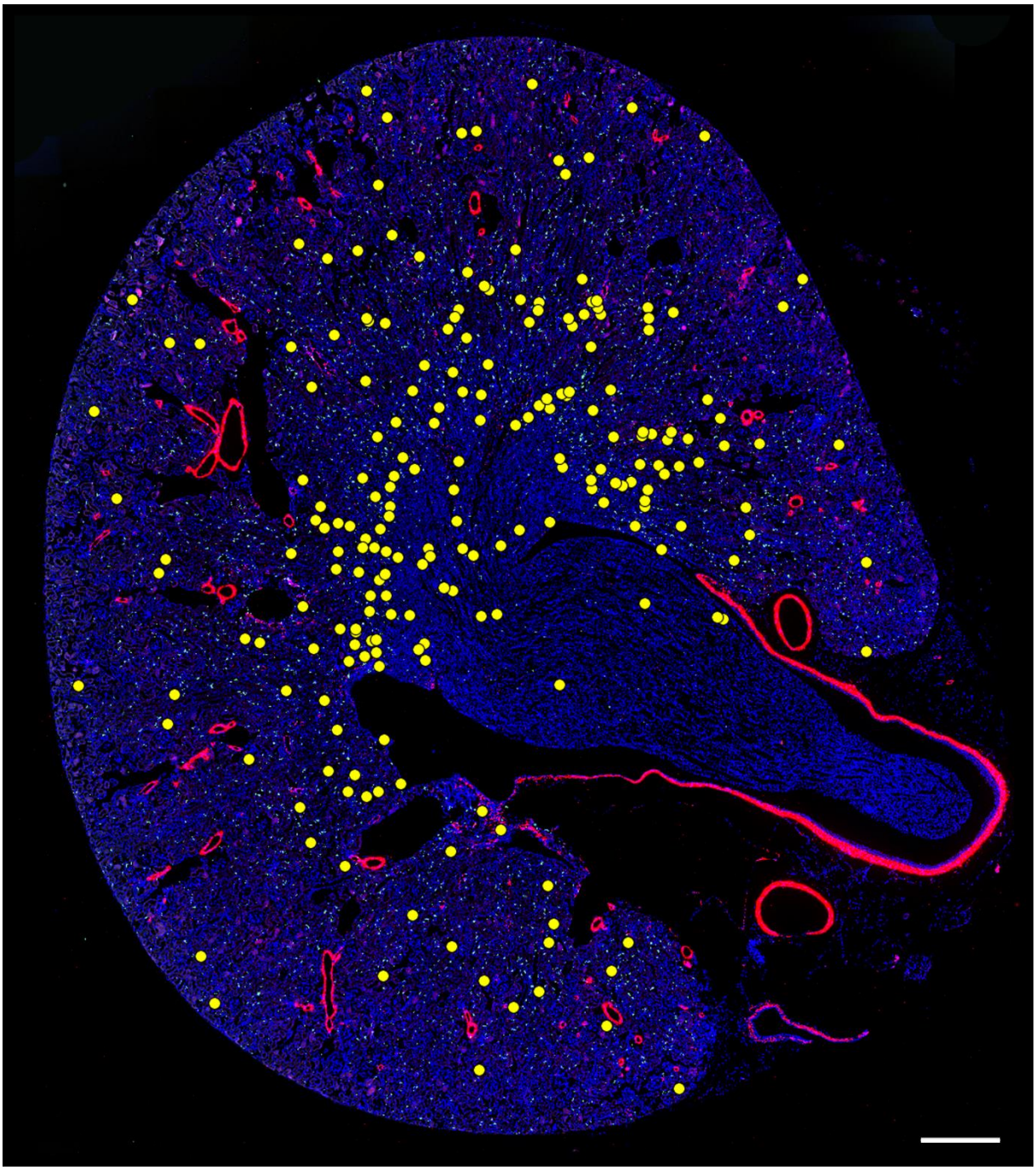

Supplementary Figure S2: Details of the outer medulla of a double in situ hybridization for EPO (green) and α-SMA (red) mRNA on an UUO kidney section of a PDGFRβ-Vhl-KO mouse. (A) Almost no EPO expression could be detected in zones strongly expressing the fibrotic marker α-SMA. EPO expression was retained in non-fibrotic areas. Scale bar = 50 µm. (B) and (C) Few EPO^{+} cells coexpressed α-SMA (arrows), but EPO mRNA expression was already lower in these cells compared to EPO expressing cells without α-SMA coexpression. Scale bar = 20 µm.

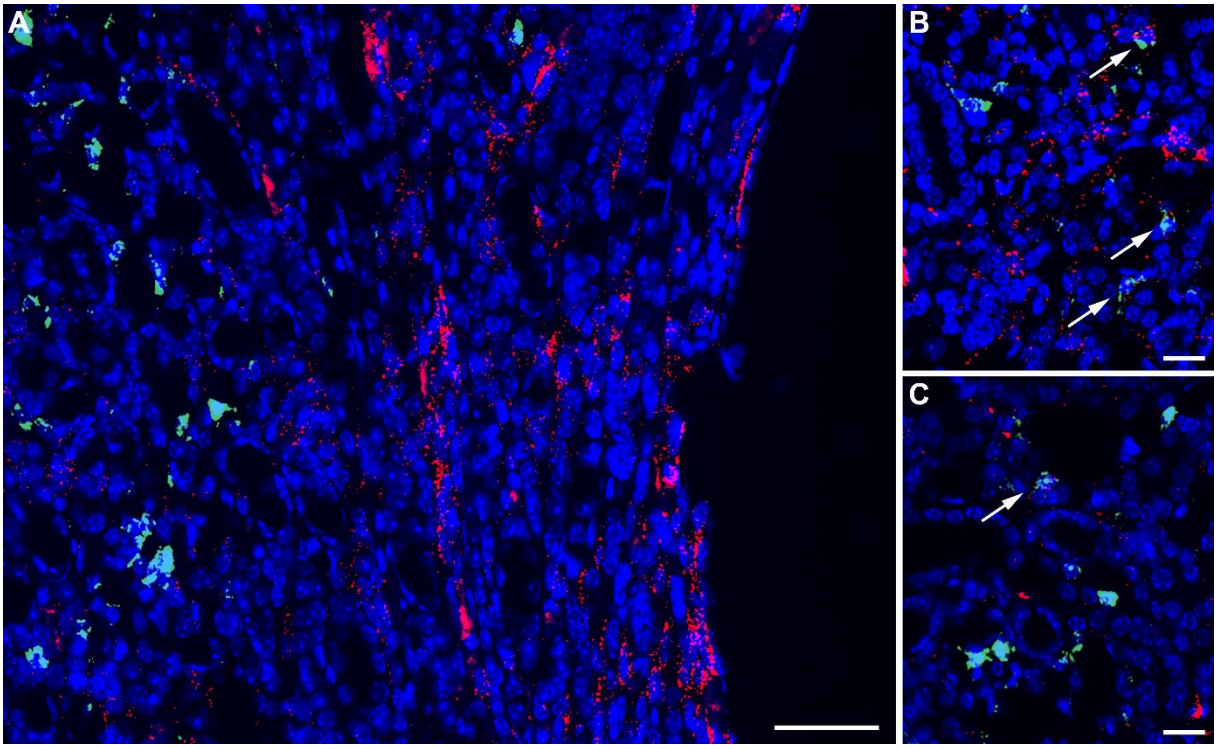

Supplementary Figure S3: Chromogenic RNAscope for EPO mRNA on kidney sections of Gli1$^{CreERT2/+}$ Vhl$^{fl/fl}$ mice in detail. EPO producing cells show the typical stellate shape. Scale bars = 20 µm.

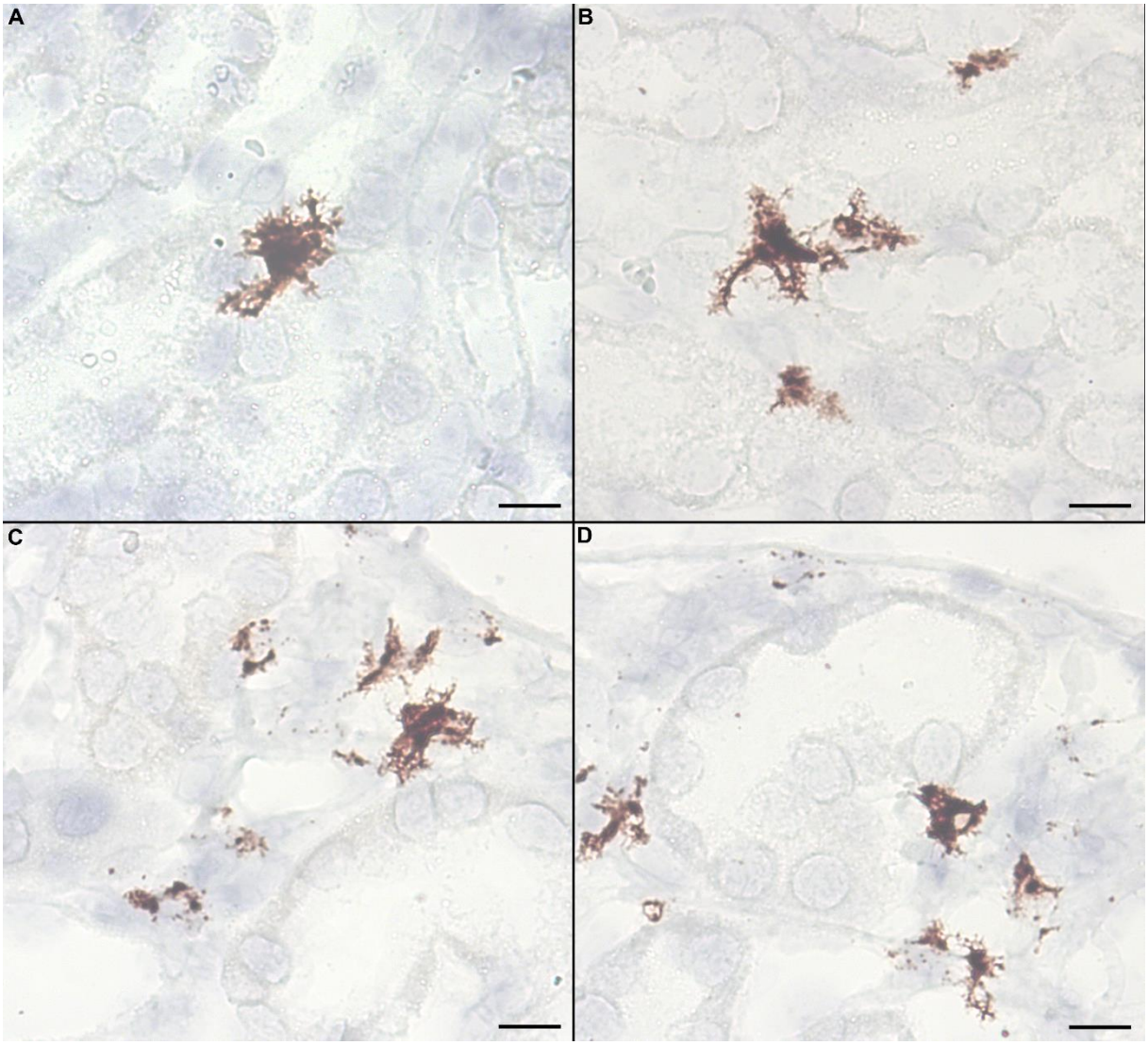

Different subpopulations of kidney interstitial cells produce erythropoietin and factors supporting tissue oxygenation in response to hypoxia *in vivo*.

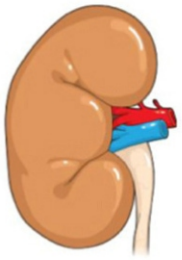

cortex

outer medulla

Normoxemia

Hypoxemia

RNAscope®

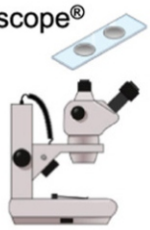

Targeted inhibition of HIF degradation

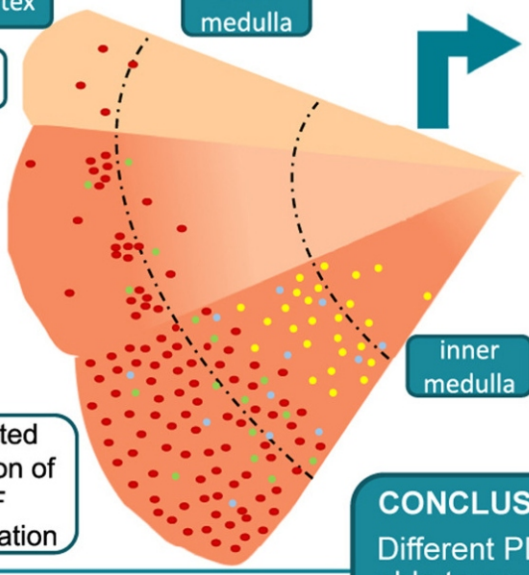

inner medulla

Different subpopulations of PDGFR-β⁺ interstitial cells expressing the additional markers CD73, Gli1, SMMHC or TNC are able to produce EPO and factors supporting tissue oxygenation such as ADM and RGS4 under different hypoxic stimuli and genetic stabilization of HIF. These subpopulations might present new targets for drugs to treat EPO deficiencies in diseased kidneys.

CONCLUSION:

Different PDGFR-β⁺ subpopulations are able to produce EPO and support tissue oxygenation in the kidney.

ISN kidney INTERNATIONAL
OFFICIAL JOURNAL OF THE INTERNATIONAL SOCIETY OF NEPHROLOGY

Broeker et al, 2020